


Quantum Brownian motion: Drude and Ohmic baths as continuum limits of the Rubin model

Avijit Das^{1,*}, Abhishek Dhar,¹ Ion Santra², Urbashi Satpathi¹, and Supurna Sinha²

¹International Center for Theoretical Sciences, Tata Institute of Fundamental Research, Bangalore 560089, India

²Raman Research Institute, Bangalore 560080, India

 (Received 2 July 2020; revised 4 November 2020; accepted 17 November 2020; published 14 December 2020)

The motion of a free quantum particle in a thermal environment is usually described by the quantum Langevin equation, where the effect of the bath is encoded through a dissipative and a noise term, related to each other via the fluctuation dissipation theorem. The quantum Langevin equation can be derived starting from a microscopic model of the thermal bath as an infinite collection of harmonic oscillators prepared in an initial equilibrium state. The spectral properties of the bath oscillators and their coupling to the particle determine the specific form of the dissipation and noise. Here we investigate in detail the well-known Rubin bath model, which consists of a one-dimensional harmonic chain with the boundary bath particle coupled to the Brownian particle. We show how in the limit of infinite bath bandwidth, we get the Drude model, and a second limit of infinite system-bath coupling gives the Ohmic model. A detailed analysis of relevant equilibrium correlation functions, such as the mean squared displacement, velocity autocorrelation functions, and response function are presented, with the aim of understanding the various temporal regimes. In particular, we discuss the quantum-to-classical crossover time scales where the mean square displacement changes from a $\sim \ln t$ to a $\sim t$ dependence. We relate our study to recent work using linear response theory to understand quantum Brownian motion.

DOI: [10.1103/PhysRevE.102.062130](https://doi.org/10.1103/PhysRevE.102.062130)

I. INTRODUCTION

A good effective description for the motion of a classical Brownian particle in a thermal environment at temperature T is given by the Langevin equation [1]. Considering motion in one dimension this is given by

$$M\dot{v} = -\gamma v + \eta(t), \quad (1)$$

where $v = \dot{x}$ is the velocity of the particle, x its position, γ the dissipation constant, and $\eta(t)$ a Gaussian noise term with mean 0 and correlations given by the fluctuation-dissipation relation $\langle \eta(t)\eta(t') \rangle = 2\gamma k_B T \delta(t - t')$. Some of the most important properties of this effective dynamics are that the particle reaches thermal equilibrium with its velocity given by the Maxwell distribution with $\langle v \rangle = 0$ and $\langle v^2 \rangle = k_B T / M$. On the other hand, the mean square displacement (MSD) shows diffusive growth at long times, $\Delta(t) = \langle [x(t) - x(0)]^2 \rangle = 2Dt$ (for $t \rightarrow \infty$), with a diffusion constant $D = k_B T / \gamma$.

The quantum version of this equation was first written by Ford, Kac, and Mazur [2]. Unlike the classical case, where the Langevin equation can be established using a purely phenomenological approach (see [3]), the quantum case requires a microscopic modeling of the heat bath. The standard model for a heat bath is to treat it as an infinite collection of oscillators which is coupled to the system of interest, namely, the Brownian particle. Eliminating the bath degrees, it can be shown that the effective dynamics of the particle is described by a quantum generalized Langevin equation, where the dissipation term has memory. A special choice of bath

leads to the so-called Ohmic form [4] of Eq. (1), with the noise correlations changed to the form

$$\langle \eta(t)\eta(t') \rangle = \frac{\gamma}{\pi} \int_0^\infty d\omega \hbar \omega [2f(\omega, T) + 1] \cos \omega(t - t'), \quad (2)$$

where $f(\omega, T) = [e^{\beta \hbar \omega} - 1]^{-1}$ is the phonon distribution function. In particular, we note that in the quantum case, the noise is always correlated and there is no Markovian limit. Interestingly, even at zero temperature there is noise arising from quantum fluctuations and it has been shown that this leads to a logarithmic growth of the MSD with time: $\Delta_t \sim (\hbar/\gamma) \ln(t\gamma/M)$ [5,6]. A peculiarity of the quantum system is that the kinetic energy of the particle diverges [7]. This divergence arises due to the contribution of high-frequency modes to the zero-point energy and can be avoided by considering a finite-bandwidth bath which leads to a damping term with memory. Since the original work in [2], quantum Brownian motion has been investigated using multiple approaches including quantum Langevin equations [8], path integral methods [9,10], equilibrium dynamical correlations [11], and linear response theory [11]. Other relevant references are [12–25].

In the present work, we discuss one of the simplest models of a quantum heat bath, the so-called Rubin bath [14]. In general it corresponds to a bath with a dissipation kernel with long-time memory, decaying as a power law. However, we point out that as special limits it leads to the Ohmic bath (the dissipation kernel is a delta function in time) and the Drude bath (the dissipation kernel decays exponentially in time) [4]. A different limiting procedure to obtain the Ohmic

*avijitds74@gmail.com

bath has been discussed in [26]. For the three bath models we discuss in detail the form of the MSD, as well as the velocity autocorrelation function and the response function, all computed in the thermal equilibrium state. We try to understand interesting physical aspects and highlight some of the qualitative differences. In recent years an approach based on linear response and fluctuation-dissipation theorem [27,28] has been used to study Brownian motion at zero temperature. We point out here that this approach is exact for the case of the Rubin model of bath.

We note that quantum Langevin equations were discussed in the most general setting in [8], where the authors first discuss these equations without resorting to a microscopic model of the bath and state the necessary conditions on the memory kernel that appears in the dissipation term. The paper then discusses how the independent oscillator model of a heat bath can be used to derive the quantum Langevin equation of the most general form. It is also pointed out that various bath models that were studied earlier are special cases of the independent oscillator model. Some of the linear coupling models that do not fall in this class do not satisfy the so-called positivity condition and are unphysical. The choice of frequencies of the bath oscillators and their coupling to the test particle fix the memory kernel and the complete dynamics. However, the work in [8] discusses the general formalism but does not investigate the interesting physical properties that are observed for specific choices of bath models. The present paper explores precisely these aspects for a particular choice of bath, namely, the Rubin model, which naturally falls in the class of independent oscillator models. For completeness here we first briefly outline the steps which lead from the Rubin model to the independent oscillator model and then to the quantum Langevin equation. As mentioned above, our other important contribution is to point out that special limits of the Rubin model lead to two physically relevant bath models, namely, the Ohmic and Drude models. The corresponding dissipation kernels for these models are simple and so are widely used, and a natural question is whether the use of these models as approximate descriptions of the original Rubin model preserves some of the observable properties. Our comparative study of the properties of various physical observables for the three models throws light on this question.

This paper is organized as follows. In Sec. II we introduce the Hamiltonian and derive the generalized Langevin equation for the system by integrating out the bath degrees of freedom. We have also discussed a continuum limit of the model and shown that the conventional and simpler models of the bath, Drude and Ohmic, emerge. In Sec. III we define the relevant correlation functions: mean square displacements, velocity autocorrelation functions, and the response functions. In Sec. IV we compute these correlations and compare the different models in detail. We end the paper with a few concluding remarks in Sec. V.

II. HAMILTONIAN AND DERIVATION OF THE GENERALIZED LANGEVIN EQUATION

Our setup, consisting of a single particle coupled to the Rubin bath, is schematically shown in Fig. 1. We consider a particle of mass M with position and momentum operators

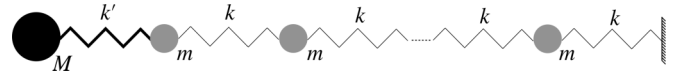


FIG. 1. Setup of the problem.

specified by x and p , respectively, while the bath consists of N particles of mass m and position and momentum operators given by $\{x_j, p_j\}$, $j = 1, 2, \dots, N$, that are coupled by harmonic springs of stiffness k . The Hamiltonian of the coupled system and bath is given by

$$\mathcal{H} = \frac{p^2}{2M} + \frac{k'}{2}(x - x_1)^2 + \sum_{n=1}^N \frac{p_n^2}{2m} + \frac{k}{2} \sum_{n=1}^N (x_n - x_{n+1})^2, \quad (3)$$

where we consider the right boundary to be fixed, $x_{N+1} = 0$. Even though our test particle (x, p) is tied to the bath, we see that in the limit $N \rightarrow \infty$, the effective motion corresponds to that of a free particle. For our analysis, it is convenient to write the above Hamiltonian in the following form:

$$\mathcal{H} = \mathcal{H}_S + \mathcal{H}_B + \mathcal{H}_{SB}, \quad (4)$$

$$\text{where } \mathcal{H}_S = \frac{p^2}{2M} + \frac{k'}{2}x^2, \quad \mathcal{H}_{SB} = -k'xx_1,$$

$$\mathcal{H}_B = \sum_{n=1}^N \frac{p_n^2}{2m} + \frac{k'}{2}x_1^2 + \frac{k}{2} \sum_{n=1}^{N-1} (x_n - x_{n+1})^2 + \frac{k}{2}x_{N+1}^2.$$

The bath Hamiltonian can be written in the compact form $\mathcal{H}_B = \mathbf{p}^T m^{-1} \mathbf{p} / 2 + \mathbf{x}^T \phi \mathbf{x} / 2$, where $\mathbf{x} = (x_1, x_2, \dots, x_N)$, $\mathbf{p} = (p_1, p_2, \dots, p_N)$, and ϕ is the force matrix. Let us consider a linear transformation $\mathbf{X} = m^{1/2} U \mathbf{x}$ and $\mathbf{P} = m^{1/2} U \mathbf{p}$, where U is an orthogonal transformation which diagonalizes the force matrix, i.e., $U \phi U^T = m \Omega^2$, where Ω^2 is the diagonal matrix with elements given by the normal-mode frequencies of the bath $\Omega^2 = \{\Omega_s^2\}$, with $s = 1, 2, \dots, N$. Note that the column vector formed by the matrix elements U_{si} gives the normal-mode eigenfunction corresponding to the eigenvalue Ω_s^2 . Using the normal-mode coordinates X_s and momenta P_s the system-bath coupling and the bath Hamiltonian can be written as

$$\mathcal{H}_{SB} = -k'xx_1 = -k' \sum_{s=1}^N C_s x X_s, \quad \text{where } C_s = m^{-1/2} U_{s1},$$

$$\mathcal{H}_B = \sum_{s=1}^N \frac{P_s^2}{2} + \frac{\Omega_s^2 X_s^2}{2}. \quad (5)$$

To derive the effective Langevin equations for the system, one starts by writing the Heisenberg equations of motion of the system and the bath degrees of freedom given by

$$M\ddot{x} = -k'x + k' \sum_{s=1}^N C_s X_s, \quad (6)$$

$$\ddot{X}_s = -\Omega_s^2 X_s + k' C_s x, \quad s = 1, 2, \dots, N. \quad (7)$$

The bath equations of motion, Eq. (7), can be solved formally, assuming the initial conditions $\{X_s(t_0), P_s(t_0)\}$ that are chosen, at time t_0 , from the Boltzmann distribution $e^{-\beta \mathcal{H}_B} / \text{Tr}[e^{-\beta \mathcal{H}_B}]$

at temperature $T = (k_B\beta)^{-1}$. This gives

$$X_s(t) = \cos\{\Omega_s(t-t_0)\}X_s(t_0) + \frac{\sin\{\Omega_s(t-t_0)\}}{\Omega_s}P_s(t_0) + k'C_s \int_{t_0}^t dt' \frac{\sin\{\Omega_s(t-t')\}}{\Omega_s}x(t'). \quad (8)$$

Plugging this into the equation of motion of the system we get

$$M\ddot{x} = -k'x + \int_{t_0}^t dt' \Sigma(t-t')x(t') + \eta(t), \quad (9)$$

where

$$\Sigma(t) = k'^2 \sum_{s=1}^N C_s^2 \frac{\sin(\Omega_s t)}{\Omega_s},$$

$$\eta(t) = k' \sum_{s=1}^N C_s \left[\cos\{\Omega_s(t-t_0)\}X_s(t_0) + \frac{\sin\{\Omega_s(t-t_0)\}}{\Omega_s}P_s(t_0) \right]. \quad (10)$$

Equation (9) is in the form of a generalized Langevin equation, with $\Sigma(t)$ the memory kernel and $\eta(t)$ the random force term. The information about the baths is completely contained in these two terms. To get a valid bath it is necessary to take the limit $N \rightarrow \infty$ since otherwise we would hit Poincaré recurrences [4]. Indeed, apparent dissipation arises in a Hamiltonian system because of the flow of energy into the infinite degrees of freedom of the bath. Next, since we are interested in equilibrium properties we take the $t_0 \rightarrow -\infty$ limit (after the $N \rightarrow \infty$ limit). This ensures that at any finite time the Brownian particle has reached thermal equilibrium. Mathematically the $t_0 \rightarrow -\infty$ limit allows us to use Fourier transforms and equilibrium correlations can be readily computed. It is instructive to write the above equations in the usual form of Langevin equations where the dissipation term involves the velocity rather than the positional degree of freedom. For this we define the dissipation kernel

$$\gamma(t) = k'^2 \sum_{s=1}^N C_s^2 \frac{\cos(\Omega_s t)}{\Omega_s^2}, \quad (11)$$

so that

$$\Sigma(t) = -\frac{d\gamma(t)}{dt}. \quad (12)$$

We plug this into Eq. (9) and perform an integration by parts. Then, using the identities $\gamma(0) = k'^2 \sum_{s=1}^N \frac{C_s^2}{\Omega_s^2} = k'^2[\phi^{-1}]_{11} = k'$ and $\gamma(\infty) = 0$, which can be proved in the $N \rightarrow \infty$ limit (for a reasonable choice of bath properties which are indeed satisfied by the baths we have considered here), and setting $t_0 \rightarrow -\infty$, we get

$$M\ddot{x} = -\int_{-\infty}^t dt' \gamma(t-t')\dot{x}(t') + \eta(t), \quad (13)$$

where we now see that the pinning potential does not appear, which is what one would like for a free particle. We now compute the bath properties in the $N \rightarrow \infty$ limit. It is useful

to define the bath spectral functions:

$$\Sigma^+(\omega) = \int_0^\infty dt \Sigma(t)e^{i\omega t} = k'^2 \sum_s \frac{C_s^2}{-(\omega+i\epsilon)^2 + \Omega_s^2},$$

$$\Gamma(\omega) = \text{Im}[\Sigma^+(\omega)]$$

$$= k'^2 \sum_s \frac{\pi C_s^2}{2\omega} [\delta(\omega - \Omega_s) + \delta(\omega + \Omega_s)]. \quad (14)$$

The statistical properties of the noise term can be obtained using the fact that at $t = t_0$ the bath is at thermal equilibrium at temperature T . Thus we find that $\langle \eta(t) \rangle = 0$ while the noise correlations are easiest to state in the Fourier domain. Defining $\tilde{\eta}(\omega) = \int_{-\infty}^\infty dt \eta(t)e^{i\omega t}$, we find [4]

$$\langle \tilde{\eta}(\omega)\tilde{\eta}(\omega') \rangle = 4\hbar\pi \Gamma(\omega)[f(\omega, T) + 1] \delta(\omega + \omega'), \quad (15)$$

where $f(\omega, T) = [e^{\beta\hbar\omega} - 1]^{-1}$ is the phonon distribution function. To compute $\Sigma^+(\omega)$, we note that it is precisely given by $k'^2 g_{1,1}^+$, where $g^+ = [-m(\omega+i\epsilon)^2 + \phi]^{-1}$ is the phonon Green's function of the heat bath and $g_{1,1}^+$ refers to its diagonal element at site $n = 1$, corresponding to the particle that is coupled to the system. The computation of $g^+(\omega)$ becomes a bit involved because of the presence of the ‘‘impurity’’ term in the bath Hamiltonian \mathcal{H}_B in Eq. (4). However, this can still be obtained explicitly and one eventually obtains [29]

$$\Sigma^+(\omega) = k'^2 \frac{e^{iq}}{k + (k' - k)e^{iq}}, \quad (16)$$

where q is given by the solution of the dispersion $\omega^2 = (2k/m)(1 - \cos q)$. In the frequency range $|\omega| \leq 2\sqrt{k/m}$, we get real values for q and then we have

$$\Gamma(\omega) = \frac{k^2 k \sin q}{|k' - k + ke^{-iq}|^2} = \frac{k^2}{k} \frac{\omega \sqrt{\frac{m}{k}} \sqrt{1 - \frac{m\omega^2}{4k}}}{\left(\frac{k'}{k}\right)^2 + \left(1 - \frac{k'}{k}\right) \frac{m\omega^2}{k}}, \quad (17)$$

while for $|\omega| > 2\sqrt{k/m}$, we get $\Gamma(\omega) = 0$. The real part of $\Sigma^+(\omega)$ is the following:

$$\text{Re}[\Sigma^+(\omega)] = \begin{cases} \frac{k^2}{k} \frac{\frac{k'}{k} - \frac{m\omega^2}{2k}}{\left(\frac{k'}{k}\right)^2 + \left(1 - \frac{k'}{k}\right) \frac{m\omega^2}{k}}, & |\omega| \leq 2\sqrt{\frac{k}{m}}; \\ \frac{k^2}{k} \frac{\frac{k'}{k} - \frac{m\omega^2}{2k} + \frac{m\omega^2}{2k} \sqrt{1 - \frac{4k}{m\omega^2}}}{\left(\frac{k'}{k}\right)^2 + \left(1 - \frac{k'}{k}\right) \frac{m\omega^2}{k}}, & |\omega| > 2\sqrt{\frac{k}{m}}. \end{cases} \quad (18)$$

Note that $\text{Re}[\Sigma^+(\omega)]$ is even with respect to ω , whereas $\Gamma(\omega) = \text{Im}[\Sigma^+(\omega)]$ is an odd function of ω . $\Sigma^+(\omega)$ decays to 0 for $|\omega| \rightarrow \infty$, which is necessary for its Fourier transform $\Sigma(t)$ to exist. These expressions of $\Sigma^+(\omega)$ become particularly simple for the case $k = k'$. Finally, we note that $\tilde{\gamma}(\omega) = \int_0^\infty dt \gamma(t)e^{i\omega t}$ is given by

$$i\omega\tilde{\gamma}(\omega) = \Sigma^+(\omega) - k'. \quad (19)$$

Continuum string limit

An interesting special case is to consider the limit corresponding to the bath's being a continuous string. This has been discussed in [26] but in a somewhat different setting.

We introduce a lattice spacing a and define the mass density $\sigma = m/a$, Young's modulus $E = ka$. The lattice parameter can be introduced in Eqs. (17) and (18) in a consistent way by substituting $m = \sigma a$, $k = E/a$, etc. The continuum limit is obtained by taking $a \rightarrow 0$, $m \rightarrow 0$, and $k \rightarrow \infty$ while keeping E and σ constant. This then gives

$$\Gamma(\omega) = \frac{\gamma_0 \omega}{1 + \omega^2 \tau^2}, \quad \tilde{\gamma}(\omega) = \frac{\gamma_0}{1 - i\omega\tau},$$

where $\gamma_0 = (\sigma E)^{1/2}$, $\tau = \gamma_0/k'$. (20)

This corresponds to the so-called *Drude* model of the bath, corresponding to a dissipation kernel $\gamma(t) = (\gamma_0/\tau)e^{-t/\tau}$. Taking the strong-coupling limit $k' \rightarrow \infty$, so that $\tau \rightarrow 0$, gives us the *Ohmic* bath model, with

$$\Gamma(\omega) = \gamma_0 \omega, \quad \tilde{\gamma}(\omega) = \gamma_0, \quad (21)$$

which gives us a memoryless dissipation kernel, $\gamma(t) = \gamma_0 \delta(t)$. We note that the presence of the phonon distribution function $f(\omega, T)$ in the quantum system ensures that the noise in Eq. (15) is still correlated and has memory. However, in the high-temperature limit, $\beta\hbar\omega \rightarrow 0$, we achieve the strictly Markovian limit $\langle \eta(t)\eta(t') \rangle = 2\gamma_0 k_B T \delta(t - t')$. The authors in [26] obtained the Ohmic bath starting from a continuum field description of the bath and using a different limiting procedure.

In the next section we discuss the behavior of various physical observables for the quantum Brownian particle that are obtained from the Rubin model and its limiting forms.

III. MEAN SQUARE DISPLACEMENT, VELOCITY AUTOCORRELATION FUNCTION, AND RESPONSE FUNCTION

In the long-time limit the particle reaches the equilibrium state and we focus on properties in this state such as the mean square displacement, velocity autocorrelation function, and response functions. The mean square displacement and the velocity autocorrelation function are defined as

$$\Delta(t) = \langle (x(t) - x(0))^2 \rangle, \quad C(t) = \frac{1}{2} \langle \{v(t), v(0)\} \rangle,$$

where $\{\dots\}$ denotes the anticommutator. The response function $R(t)$ and velocity response function $\bar{R}(t)$ are defined through the equations for the average displacement and average velocity in the presence of a driving force $f(t)$,

$$\langle \Delta x(t) \rangle := \langle x(t) \rangle_f - \langle x \rangle_{f=0} = \int_{-\infty}^t dt' R(t - t') f(t'), \quad (22)$$

$$\langle v(t) \rangle = \int_{-\infty}^t dt' \bar{R}(t - t') f(t'), \quad (23)$$

where $\langle \dots \rangle_f$ is the expectation value in the presence of the force and $\langle \dots \rangle_{f=0}$ in the absence of it. By definition, $\bar{R}(t) = \dot{R}(t)$. All three of these quantities can be obtained through the Fourier transform solution of Eq. (9) (after taking the limits $N \rightarrow \infty$ and $t_0 \rightarrow -\infty$) and Eq. (13). The transform $\tilde{x}(\omega) = \int_{-\infty}^{\infty} dt x(t) e^{i\omega t}$ is given by

$$\tilde{x}(\omega) = G(\omega) \tilde{\eta}(\omega), \quad \text{where} \quad (24)$$

$$G(\omega) = \frac{1}{-M\omega^2 + k' - \Sigma^+(\omega)} = \frac{1}{-M\omega^2 - i\omega\tilde{\gamma}(\omega)}. \quad (25)$$

Using this and the noise properties leads immediately to

$$\begin{aligned} \Delta(t) &= 2\langle x^2(0) \rangle - \langle \{x(t), x(0)\} \rangle \\ &= \frac{\hbar}{\pi} \int_{-\infty}^{\infty} d\omega \coth(\beta\hbar\omega/2) \Gamma(\omega) G(\omega) G(-\omega) (1 - e^{-i\omega t}) \\ &= \frac{2\hbar}{\pi} \int_0^{\infty} d\omega \coth(\beta\hbar\omega/2) \Gamma(\omega) G(\omega) G(-\omega) (1 - \cos \omega t) \\ &= \frac{2\hbar}{\pi} \int_0^{\infty} d\omega \coth(\beta\hbar\omega/2) \text{Im}[G(\omega)] (1 - \cos \omega t), \end{aligned} \quad (26)$$

$$(27)$$

where we have used the Green's function identity $\Gamma(\omega)G(\omega)G(-\omega) = [G(\omega) - G(-\omega)]/(2i)$.

The velocity autocorrelation function can be obtained from $\Delta(t)$ as

$$\begin{aligned} C(t) &= \frac{1}{2} \frac{d^2 \Delta(t)}{dt^2} \\ &= \frac{\hbar}{\pi} \int_0^{\infty} d\omega \coth(\beta\hbar\omega/2) \Gamma(\omega) G(\omega) G(-\omega) \omega^2 \cos \omega t \\ &= \frac{\hbar}{\pi} \int_0^{\infty} d\omega \coth(\beta\hbar\omega/2) \text{Im}[G(\omega)] \omega^2 \cos \omega t. \end{aligned} \quad (29)$$

The velocity response function is given by

$$\bar{R}(t) = \frac{1}{2\pi} \int_{-\infty}^{\infty} d\omega \frac{e^{-i\omega t}}{-i\omega M + \tilde{\gamma}(\omega)} \quad (30)$$

$$= \frac{1}{2\pi} \int_{-\infty}^{\infty} d\omega (-i\omega) G(\omega) e^{-i\omega t}, \quad (31)$$

whereas the relation $\bar{R}(t) = \dot{R}(t)$ gives us an expression of the position response function,

$$\begin{aligned} R(t) &= \int_0^t dt' \bar{R}(t') = \frac{1}{2\pi} \int_{-\infty}^{\infty} d\omega G(\omega) (e^{-i\omega t} - 1) \\ &= \frac{1}{\pi} \int_0^{\infty} d\omega [\text{Re}[G(\omega)] [\cos(\omega t) - 1] \\ &\quad + \text{Im}[G(\omega)] \sin(\omega t)], \end{aligned} \quad (32)$$

$$(33)$$

where we have used the symmetry properties of $G(\omega)$: $\text{Re}[G(-\omega)] = \text{Re}[G(\omega)]$ and $\text{Im}[G(-\omega)] = -\text{Im}[G(\omega)]$. On the other hand, the positional correlation function is given by

$$\begin{aligned} \frac{1}{i\hbar} \langle [x(t), x(0)] \rangle &= \frac{1}{\pi i} \int_{-\infty}^{\infty} d\omega \Gamma(\omega) G(\omega) G(-\omega) e^{-i\omega t} \\ &= \frac{-1}{2\pi} \int_{-\infty}^{\infty} d\omega [G(\omega) - G(-\omega)] e^{-i\omega t} \\ &= \frac{-1}{\pi} \int_{-\infty}^{\infty} d\omega \text{Im}[G(\omega)] \sin(\omega t). \end{aligned} \quad (34)$$

Using the Kramer's Kronig identity, $\int_{-\infty}^{\infty} d\omega \text{Im}[G(\omega)] \sin(\omega t) = \int_{-\infty}^{\infty} d\omega \text{Re}[G(\omega)] [\cos(\omega t) - 1]$, we verify explicitly that the linear response formula,

$$R(t) = -\frac{1}{i\hbar} \langle [x(t), x(0)] \rangle, \quad (35)$$

holds exactly. This is expected since the dynamics of the system and bath is completely linear.

IV. COMPARISON OF THE FORMS OF $\gamma(t)$, $\Delta(t)$, AND $C(t)$ FOR THE THREE MODELS

A. Form of $\gamma(t)$

1. Rubin model

In this case one can obtain the expression of $\tilde{\gamma}(\omega)$ using Eq. (16) and Eq. (19),

$$\text{Re}[\tilde{\gamma}(\omega)] = \frac{k'^2}{k} \sqrt{\frac{m}{k}} \frac{\sqrt{1 - \frac{m\omega^2}{4k}}}{\left(\frac{k'}{k}\right)^2 + \left(1 - \frac{k'}{k}\right)\left(\frac{m\omega^2}{k}\right)}, \quad (36)$$

for $|\omega| \leq 2\sqrt{\frac{k}{m}}$ and $\text{Re}[\tilde{\gamma}(\omega)] = 0$ for $|\omega| > 2\sqrt{\frac{k}{m}}$.

$$\text{Im}[\tilde{\gamma}(\omega)] = m\omega \frac{\frac{k'}{k} - \frac{1}{2}\left(\frac{k'}{k}\right)^2}{\left(\frac{k'}{k}\right)^2 + \left(1 - \frac{k'}{k}\right)\left(\frac{m\omega^2}{k}\right)} \quad (37)$$

for $|\omega| \leq 2\sqrt{\frac{k}{m}}$ and

$$\text{Im}[\tilde{\gamma}(\omega)] = m\omega \frac{\frac{k'}{k} - \frac{1}{2}\left(\frac{k'}{k}\right)^2 \left[1 + \sqrt{1 - \frac{4k}{m\omega^2}}\right]}{\left(\frac{k'}{k}\right)^2 + \left(1 - \frac{k'}{k}\right)\left(\frac{m\omega^2}{k}\right)} \quad (38)$$

for $|\omega| > 2\sqrt{\frac{k}{m}}$.

Note that $\text{Re}[\tilde{\gamma}(\omega)]$ is an odd function of ω , while $\text{Im}[\tilde{\gamma}(\omega)]$ is even. This property is common for various response functions in physical systems. For the special case $k = k'$, it is possible to evaluate $\gamma(t) = \frac{1}{2\pi} \int_{-\infty}^{\infty} d\omega \tilde{\gamma}(\omega) e^{-i\omega t}$ to obtain

$$\gamma(t) = \frac{\sqrt{km} J_1\left(2\sqrt{\frac{k}{m}} t\right)}{t}, \quad (39)$$

where J_n is the Bessel function of the first kind. Since $J_n(x) \sim \sqrt{\frac{2}{\pi x}} \cos\left[x - (n + 1/2)\frac{\pi}{2}\right]$ at large x , we get the leading-order asymptotic behavior $\gamma(t) \sim t^{-3/2}$. This leading asymptotic form can be seen as arising from the branch point at $\omega = 2\sqrt{k/m}$ in the integrand in Eq. (36). For the general case, $k \neq k'$, we note that the integrand has additional poles at

$\omega = k'/\sqrt{m(k' - k)}$. For $k > k'$, this is imaginary and gives rise to an exponentially decaying part in $\gamma(t)$. Thus we expect that for $k > k'$, $\gamma(t)$ should initially have a fast exponential decay $\sim e^{-\omega_p t}$, where $\omega_p = k'/\sqrt{m(k' - k)}$. After a time scale $t_c \approx 2\pi/\omega_p$, this is followed by a $\sim t^{-3/2}$ decay. This feature is clearly seen in the numerical evaluation of $\gamma(t)$ and is presented in Fig. 2 for two parameter sets. In [30] the authors have addressed this question of crossover time scales in a similar system heuristically.

2. Drude bath and Ohmic bath limits

From Eq. (20) one obtains $\gamma(t) = \frac{\gamma_0}{\tau} e^{-t/\tau}$ and $\Sigma(t) = \frac{\gamma_0}{\tau^2} e^{-t/\tau}$. An Ohmic bath is obtained simply taking the limit $\tau \rightarrow 0$ and gives $\gamma(t) = \gamma_0 \delta(t)$.

In Fig. 3 we show a comparison of the forms of $\gamma(t)$ obtained from the Rubin and Drude models. As expected we see that for the weak-coupling case ($k' = 0.5$), we expect an exponentially decaying regime for the Rubin model over the time scale $t_c \approx 2\pi/\omega_p \approx 25.3$, and here we see agreement with the Drude model. On the other hand, when $k' = 4.0$, we see that $t_c \approx 1.5$, and correspondingly one finds that there is no regime where the Drude approximation is good.

We next explore the question how well the behavior of other physical observables such as $\Delta(t)$ and $C(t)$ are reproduced by the Drude and Ohmic approximations.

B. Form of $\Delta(t)$

To compute $\Delta(t)$, $C(t)$, and $R(t)$ we need information on $\text{Im}[G(\omega)]$. Using Eqs. (25), (36), and (37) we get

$$\begin{aligned} \text{Im}[G(\omega)] &= \frac{\frac{k'^2}{k} \frac{1}{m\omega^3} \sqrt{\frac{1}{mk}} \sqrt{1 - \frac{m\omega^2}{4k}} \left(\left[\frac{k'}{k}\right]^2 + \frac{m\omega^2}{k} \left[1 - \frac{k'}{k}\right]\right)}{\left[\frac{M\omega^2}{k} \left[1 - \frac{k'}{k}\right] + \frac{k'^2}{k^2} \left[\frac{M}{m} + \frac{1}{2}\right] - \frac{k'}{k}\right]^2 + \frac{k'^4}{m\omega^2 k^3} \left[1 - \frac{m\omega^2}{4k}\right]} \end{aligned} \quad (40)$$

for $|\omega| \leq 2\sqrt{k/m}$ and 0 for $|\omega| > 2\sqrt{k/m}$.

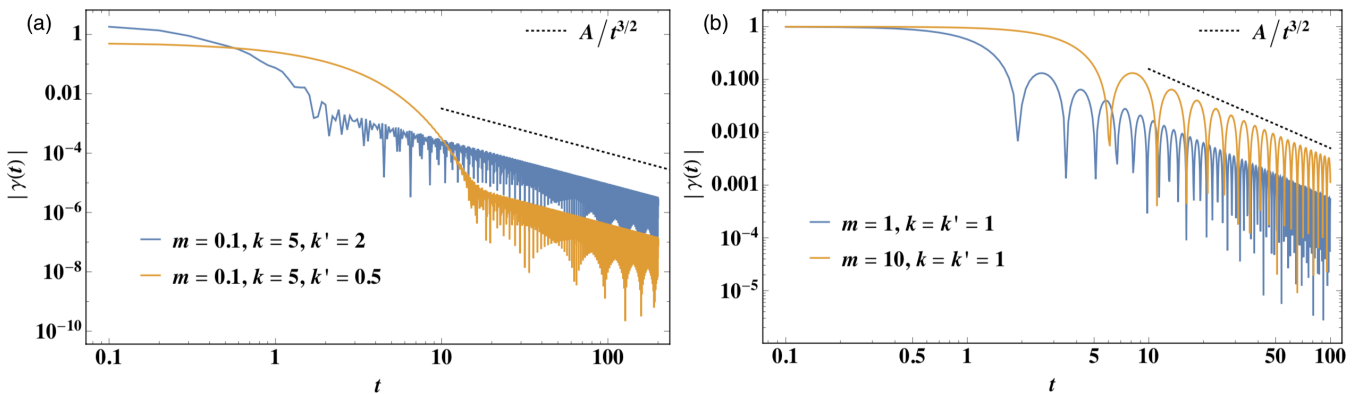


FIG. 2. Rubin model. Log-log plot of $|\gamma(t)|$ for a set of values of m , k , and k' to show that $\gamma(t)$ initially decays rapidly and then as a power law, $\sim t^{-3/2}$. We propose that the crossover time, t^* , can be estimated from the location of the branch point of $\tilde{\gamma}(\omega)$: $t^* \propto \sqrt{\frac{m}{k'}\left(\frac{k}{k'} - 1\right)}$ when $k > k'$ and $t^* \propto \sqrt{\frac{m}{k}}$ when $k \leq k'$. (a) $k > k'$; if we decrease just k' by a factor of 4, keeping other parameters fixed, t^* increases by 4 times. (b) $k = k'$; m is increased by 10 times, which results in a shift of t^* by a factor of $\sqrt{10}$. These observations support our claim about the crossover time.

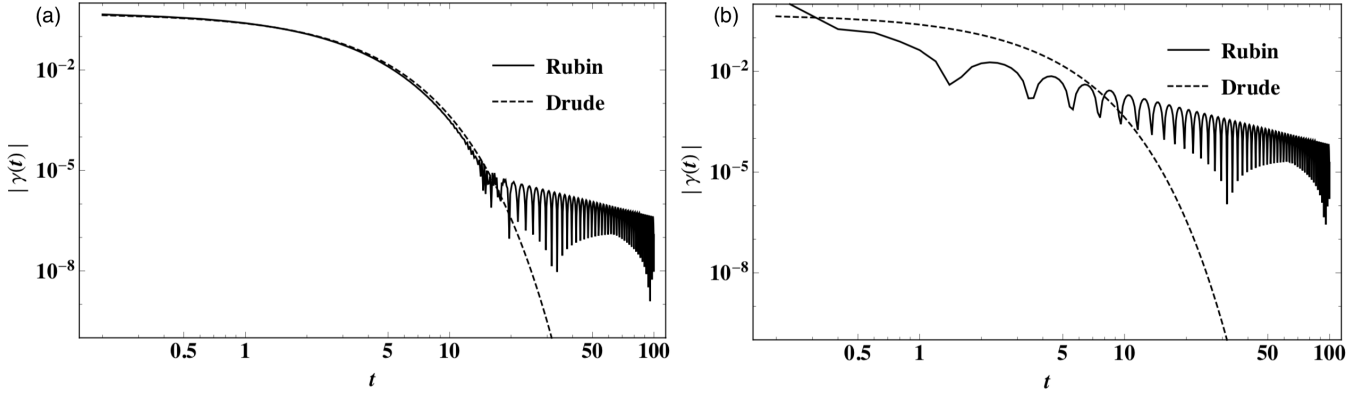


FIG. 3. Comparison of $\gamma(t)$ between the Rubin and the Drude models: (a) weak-coupling case, $k' = 0.5$; (b) strong-coupling case with $k' = 4.0$. Other parameters are taken as $M = 1$, $m = 0.1$, $k = 5$. These data support the fact that the Drude approximation of the Rubin bath is good when k is large but k' is not. If both k and k' are made large, the Ohmic approximation is better than the Drude.

The corresponding form for the Drude bath is given by

$$\text{Im}[G(\omega)] = \frac{\gamma_0}{\omega[M^2\omega^2 + (M\omega^2\tau - \gamma_0)^2]}. \quad (41)$$

An Ohmic bath is obtained from the above expression by letting $\tau \rightarrow 0$. Most of the integrals of $\Delta(t)$ and $C(t)$ for the Rubin model are intractable analytically but can be done numerically to extract some limiting behaviors.

Numerical results from the evaluation of the integral, Eq. (27), and a comparison with results from the corresponding Drude and Ohmic limits is shown in Figs. 4, 5, 6, 7, and 8. Some of the interesting observations can be summarized as follows:

(1) At long times we see a linear growth of $\Delta(t)$ with time, at all finite temperatures, as expected for a diffusive system. We note that the integrand has an oscillatory factor $[1 - \cos(\omega t)]$, so at large t the major contribution to the integral comes from $\omega \ll 1/t$. Hence, for any nonvan-

ishing β , we take $\coth(\frac{\beta\hbar\omega}{2}) \rightarrow \frac{2}{\beta\hbar\omega}$ to get (in the $t \rightarrow \infty$ limit)

$$\begin{aligned} \Delta(t) &= \frac{4}{\pi\beta} \int_0^\infty d\omega (\omega \text{Im}[G(\omega)])_{\omega \rightarrow 0} \frac{1 - \cos(\omega t)}{\omega^2} \\ &= \frac{2}{\beta\sqrt{mk}} t = 2Dt, \end{aligned} \quad (42)$$

where

$$D = \frac{1}{\beta\sqrt{mk}} = \frac{k_B T}{\gamma_0} \quad (43)$$

can be identified as the usual diffusion constant satisfying the Stokes-Einstein relation. In Figs. 7(b) and 4(b), we verify that $\Delta(t)/t$ does converge to this limit at finite temperatures. As shown in these figures, the long-time asymptotics of $\Delta(t)$ and the diffusion constant are thus correctly obtained by both the Drude and the Ohmic limits. The diffusion constant values are specified in Fig. 7(b) for two β values and other parameter choices. Note that D vanishes at zero temperature ($\beta = \infty$), which is also clear from Fig. 7(b).

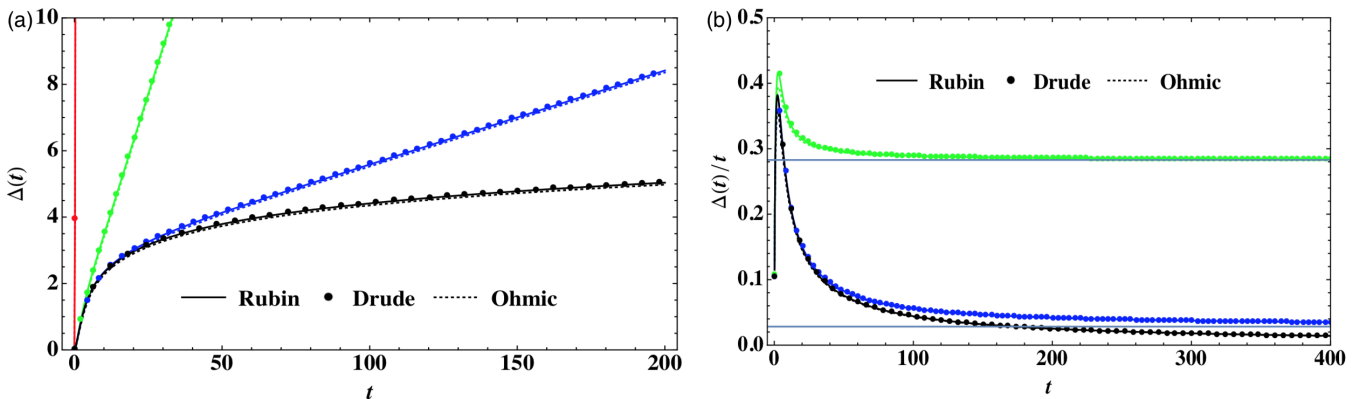


FIG. 4. (a) Comparison of $\Delta(t)$ between the Rubin, Drude, and Ohmic models. β values (from left to right) are 0.01, 10, 100, and ∞ . (b) For β values 10, 100, and ∞ (top to bottom), we plot $\Delta(t)/t$. Other parameters are taken as $M = 1$, $m = 0.1$, $k = 5$, $k' = 4.0$. This figure is the counterpart of Fig. 7 with k and k' both large. The saturation values (0.283 and 0.0283) are indicated. We see agreement between the three models compared to Fig. 7.

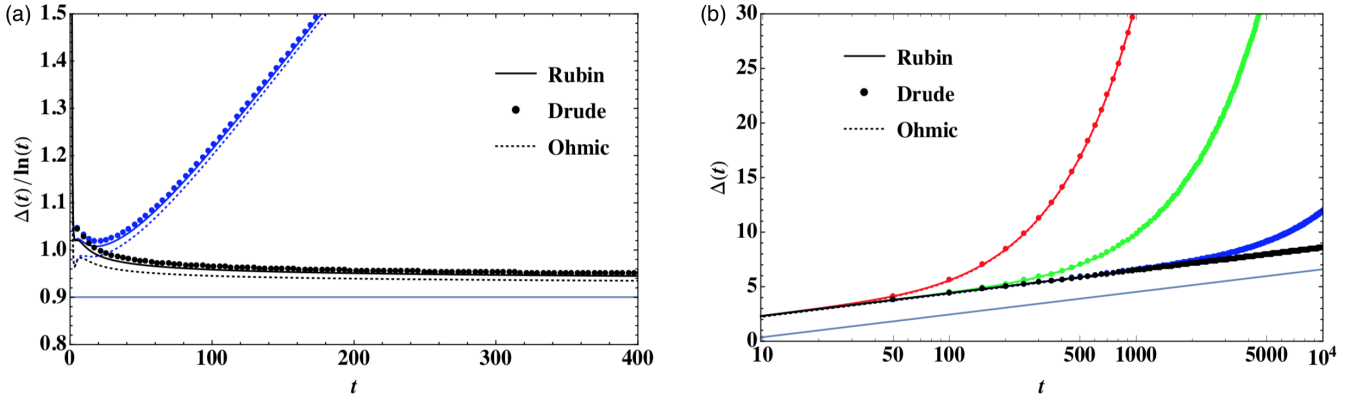


FIG. 5. (a) Comparison of $\Delta(t)/\ln(t)$ between the Rubin, Drude, and Ohmic models for $\beta = 10$ and ∞ (top and bottom) at linear scale. (b) $\Delta(t)$ at log-linear scale for $\beta = 100, 500, 5000$, and ∞ (top to bottom). Other parameters were taken as $M = 1, m = 0.1, k = 5, k' = 4.0$. Note the match between different models, as k and k' both are large, in contrast to Fig. 8. From Eq. (44) the prefactor of $\ln(t)$ is $2\hbar/\pi\gamma_0 = 0.9$, which is indicated in both (a) and (b).

(2) At zero temperature ($\beta \rightarrow \infty$) we find that $\Delta(t)$ has a slower logarithmic growth at large times. In this quantum regime we have $\coth(\frac{\beta\hbar\omega}{2}) = 1$ and the integrals simplify. As before, we have to consider only the small ω contribution to the integral for the large-time asymptotic behavior of $\Delta(t)$:

$$\begin{aligned} \Delta(t) &\simeq \frac{2\hbar}{\pi} \int_0^{2\sqrt{\frac{k}{m}}} d\omega (\omega \text{Im}[G(\omega)])_{\omega \rightarrow 0} \frac{1 - \cos(\omega t)}{\omega} \\ &\simeq \frac{2\hbar}{\pi\gamma_0} \ln(t). \end{aligned} \quad (44)$$

In Fig. 8(a) we verify this form and the value of the prefactor of $\ln(t)$. We see that the Rubin, Drude, and Ohmic models reproduce the logarithmic growth. The prefactors of $\ln(t)$ are the same, which is evident in Fig. 8(b) and Fig. 5(b), as the slopes of different models of the linear regime are the same at log-linear scale. Note that there must be a time scale included in the argument of the log for dimensional constraints. The

log behavior can be represented by $\Delta(t) \sim A + B \ln(t)$, which implies that $\Delta(t)/\ln(t) \sim A/\ln(t) + B$. As $\ln(t)$ is a slowly varying (increasing) function of t , there is a slow convergence to the model independent prefactor B of $\ln(t)$, as shown in Fig. 8(a) and Fig. 5(a). The chosen parameters are mostly $M = 1, m = 0.1, k = 5$, and $k' = 0.5$ or 4 throughout the numerical data presented here for various β values. For Drude and Ohmic baths, γ_0 and τ are also chosen correspondingly [see Eq. (20)].

(3) At finite temperatures, the crossover from the quantum (logarithmic growth) to the classical (linear growth) takes place at the time scale $t_{qc} \sim \beta\hbar$. We study this time scale in Fig. 8(b) and Fig. 5(b), by plotting the $\Delta(t)$ for various β values keeping $\hbar = 1$. On the log-linear scale, the log behavior of $\Delta(t)$ is represented by a linear regime which persists up to a time scale of the order of $\beta\hbar$.

(4) Finally, we discuss the short-time behavior. At high temperatures, we approximate $\frac{1 - \cos(\omega t)}{\omega^2} \sim t^2/2$ and

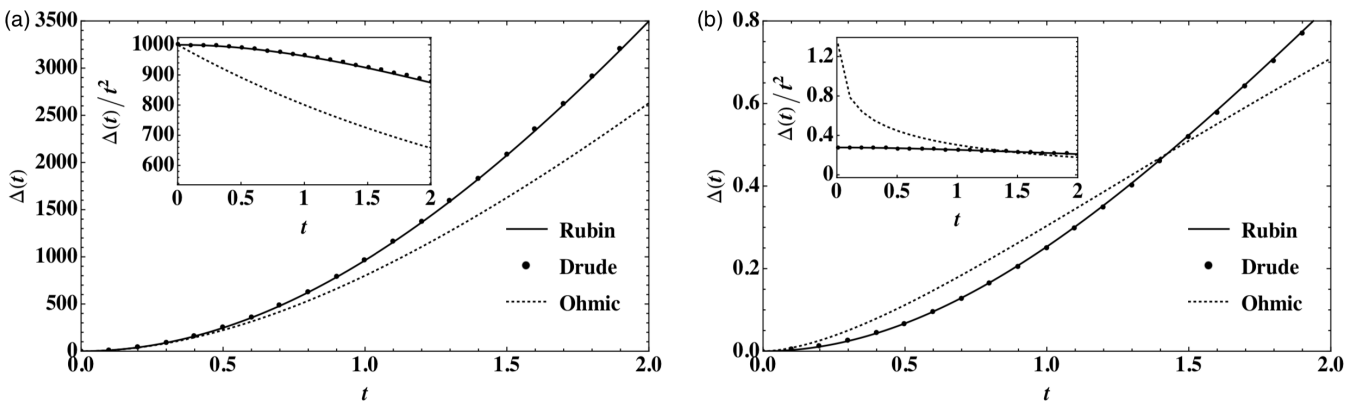


FIG. 6. Comparison of $\Delta(t)$ between the Rubin, Drude, and Ohmic models at short times. (a) $\beta = 0.001$. We can see that at high temperatures $\Delta(t)$ behaves as $\sim t^2$ for all three models. The correction to the t^2 behavior for the Ohmic case is t^3 , which is evident in the inset. (b) $\beta = 100$. At low and finite temperatures, the short-time behavior is $\sim -t^2 \ln(t)$ for the Ohmic bath, whereas it is $\sim t^2$ for the Rubin and Drude baths. Other parameters are $M = 1, m = 0.1, k = 5, k' = 0.5$. Note that the log divergence of $C(0)$ for the Ohmic case is present at any finite temperature and diminishes for $\beta\hbar$ equal to 0, which is hard to achieve numerically. Thus in the data presented in (a) for the Ohmic case, we have first taken the classical limit and then performed the integral.

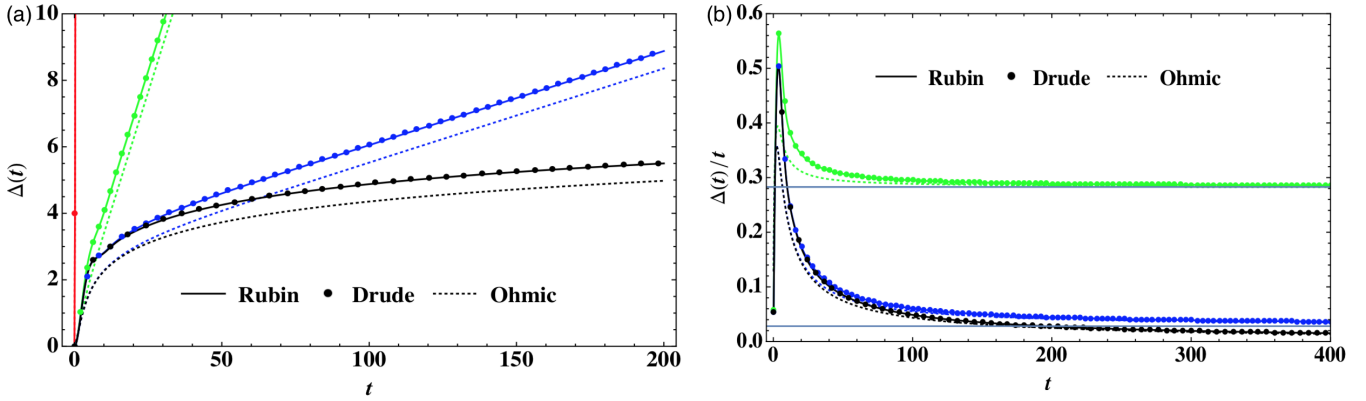


FIG. 7. Comparison of $\Delta(t)$ between the Rubin, Drude, and Ohmic models: (a) β values are 0.01, 10, 100, and ∞ (left to right). (b) For β values 10, 100, and ∞ (top to bottom) we plot $\Delta(t)/t$. We verify the asymptotic formulas presented in Eqs. (42) and (43) at finite temperatures. At $\beta = 10$ the saturation value is $2D = 2/\beta\sqrt{km} = 0.283$ and at $\beta = 100$ it is 0.0283, which match with the data. These saturation values are indicated. Other parameters were taken as $M = 1$, $m = 0.1$, $k = 5$, $k' = 0.5$.

coth $(\frac{\beta\hbar\omega}{2}) \sim \frac{2}{\beta\hbar\omega}$, to obtain

$$\Delta(t) \simeq \frac{2}{\pi\beta} t^2 \int_0^{2\sqrt{\frac{k}{m}}} d\omega \omega \text{Im}[G(\omega)] \sim c \frac{k_B T}{M} t^2, \quad (45)$$

where c is a dimensionless constant. The ballistic growth can be simply understood as that of a thermal particle with $\langle v^2 \rangle = k_B T/M$. On the other hand, at zero temperature, we get

$$\Delta(t) \simeq c' \frac{\hbar k^{1/2}}{M^{3/2}} t^2, \quad (46)$$

where $c' = [2M^{3/2}/(k^{1/2}\pi)] \int_0^{2\sqrt{k/m}} d\omega \omega^2 \text{Im}[G(\omega)]$ is a dimensionless constant. The ballistic growth in this case roughly corresponds to a particle with velocity fluctuations determined by the zero-point energy so that $\langle v^2 \rangle = \hbar(k/M)^{1/2}/M$.

As presented in Fig. 6(a), we see that in the high-temperature limit, all three models show t^2 behavior with the same prefactor. This is consistent with the equipartition interpretation.

At zero temperature or any finite temperature, the Drude and Rubin models have the expected form of (46) with the same prefactor, while the Ohmic model has a logarithmic correction given by

$$\Delta(t) \simeq -\frac{\hbar\gamma_0}{M^2\pi} t^2 \ln(\gamma_0 t/M) + O[t^4 \ln(t)]. \quad (47)$$

The data are presented in Fig. 6(b).

C. Form of $C(t)$

$C(t)$ is obtained from $\Delta(t)$ by taking two time derivatives [Eq. (28)]. Numerical data are presented in Fig. 9. Some important features are the following:

(1) One general feature is a damped oscillatory behavior in most parameter regimes. We can also see the agreement between the three models when both k and k' are chosen to be large. However, there is a significant deviation of the Ohmic bath near $t = 0$.

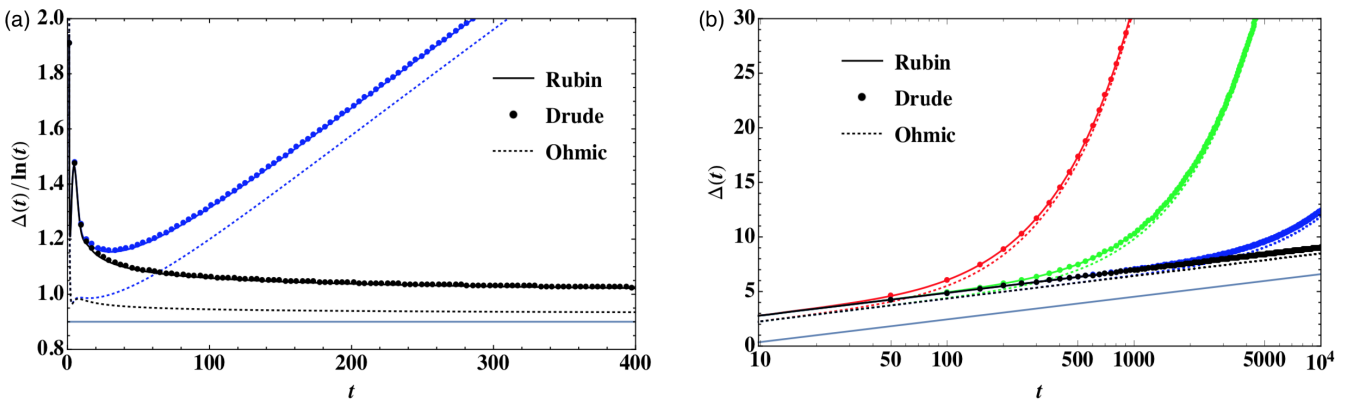


FIG. 8. (a) Comparison of $\Delta(t)/\ln(t)$ between the Rubin, Drude, and Ohmic models. $\beta = 10$ and ∞ (top and bottom) at linear scale. (b) $\Delta(t)$ at log-linear scale for $\beta = 100, 500, 5000$, and ∞ (top to bottom). This figure indicates the log behavior of $\Delta(t)$ for all three models with the same prefactors (slopes of the linear region) up to a time scale of the order of $\sim\beta\hbar$. Beyond this time scale $\Delta(t)$ behaves linearly in time, which causes exponential growth at log-linear scale. Other parameters were taken as $M = 1$, $m = 0.1$, $k = 5$, $k' = 0.5$. We note that the Rubin and Drude models match well but the Ohmic model deviates. This occurs because k is large but k' is relatively small. However, as (b) suggests, the prefactors of $\ln(t)$ are the same for these models and hence there is a slow convergence of the data at (a) for $\beta = \infty$. From Eq. (44) the prefactor of $\ln(t)$ is $2\hbar/\pi\gamma_0 = 0.9$, which is indicated in both (a) and (b).

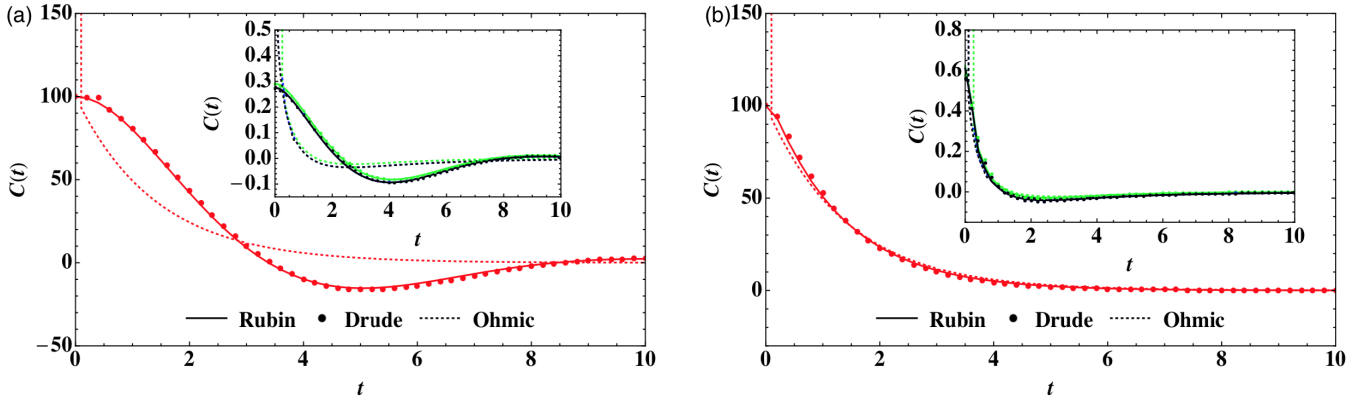


FIG. 9. Comparison of $C(t)$ between the Rubin, Drude, and Ohmic baths: (a) $M = 1$, $m = 0.1$, $k = 5$, $k' = 0.5$, $\beta = 0.01$. Inset: $\beta = 10$, 100, and ∞ (top to bottom). (b) $M = 1$, $m = 0.1$, $k = 5$, $k' = 4$, $\beta = 0.01$. Inset: $\beta = 10$, 100, and ∞ (top to bottom). As in the case of $\Delta(t)$, there is better agreement between the Rubin and the Drude models than the Ohmic bath when the k value is sufficiently large but k' is not. And all three models coincide when k and k' both are chosen to be large. Near $t = 0$, there is a log divergence, which is only present in the Ohmic case [see Eq. (48)] and this deviation is always visible near $t = 0$.

(2) In the case of the Rubin and Drude models, at all temperatures, $\Delta(t)$ behaves as $\sim t^2$ near $t = 0$, which gives a finite value of $C(0)$. Note that $C(0) = k_B T/M$ in the classical regime and $C(0) = \hbar(k/M)^{1/2}/M$ in the quantum regime. $C(t) \sim C(0) + O(t^2)$ at small times.

However, for the Ohmic bath, from Eq. (47) we get

$$C(t) \simeq -\frac{\gamma_0 \hbar}{\pi m^2} \ln(\gamma_0 t/M) + O[t^2 \ln(t)]. \quad (48)$$

This log divergence near $t = 0$ explains the deviation from other bath models shown in Fig. 9. Although Eq. (47) was derived for low temperatures, this log divergence occurs at any finite temperature. In the classical limit, i.e., when $\beta \hbar = 0$, one gets an exponential decay of the velocity autocorrelation.

(3) In the previous section, we obtained the leading-order term for $\Delta(t)$, which behaves as $\sim t$ in the large-time limit at any finite temperature. If we take double derivatives naively, it does not lead to the correct leading-order asymptote of $C(t)$. In a detailed calculation (to be published), we have shown that the correction to this linear behavior is $\sim e^{-ct}$ for the Drude and Ohmic models and $\sim \cos(\omega t)/t^{3/2}$ for the Rubin bath. Thus the large-time behavior ($t \gg \beta \hbar$) of $C(t)$ is $\sim e^{-ct}$ for the Drude and Ohmic baths and $\sim \cos(t)/t^{3/2}$ for the Rubin. At zero temperature or $t \ll \beta \hbar$ the leading-order behaviors are $\sim 1/t^2$ for all three models.

D. Form of $R(t)$

Using Eq. (32) we obtain

$$R(t) = [1 - \exp(-\gamma_0 t/m)]/\gamma_0 \quad (49)$$

for the Ohmic model. For the Drude model, the integrals can also be evaluated exactly and $R(t)$ takes a similar functional form. The general feature that $R(t)$ increases initially and then saturates to a value is present in all models and parameter regimes. This behavior physically describes the fact that if we perturb the Brownian particle, it will initially have a directional displacement before it becomes completely random. For the Rubin bath the integrals are intractable. Data from numerical integration for all three modes are shown in Fig. 10.

Numerical details

To perform the integrals numerically MATHEMATICA has been used extensively, especially the NIntegrate command. To obtain the analytical and asymptotic formulas, do the summations, etc., commands like Integrate, AsymptoticIntegrate, Series, FullSimplify, etc., of MATHEMATICA have been used in particular.

V. SUMMARY AND DISCUSSION

In this paper we study in detail the well-known Rubin bath model, which consists of a one-dimensional semi-infinite harmonic chain with a boundary bath particle coupled to a test particle, which is then shown to effectively execute Brownian motion. We point out two interesting and important limits of the Rubin model: (i) the Drude model, which is obtained in the infinite bath bandwidth limit of the Rubin model, and (ii) the Ohmic model, which, in addition to an infinite bath bandwidth, also needs the limit of infinite system-bath coupling. For the Rubin model and the special limiting cases, we analyze in detail the temporal dependence of the mean square displacement, the velocity autocorrelation function, and the response function. In addition, we study the crossover behavior of the dissipation kernel $\gamma(t)$ from an exponentially decaying behavior at short times to an oscillatory power-law ($\sim t^{-3/2}$) decaying behavior at larger times.

Taking the special limits of either the Drude or the Ohmic bath is useful since the bath kernels are much simpler and the mathematical analysis becomes considerably simpler. In real physical situations one might have large but finite bath bandwidths and system-bath couplings. One important question in these situations is how closely physical properties are reproduced when we ignore the fact that the original Rubin bath kernel has long-time power-law tails. Our numerical results show that many properties are indeed accurately reproduced by the approximate models. For example, we show that even though the Rubin bath has a memory kernel with power-law tails, which is completely different from the exponential decay for the Debye model, this does not affect the asymptotic form of the mean square displacement. In particular, we discuss the

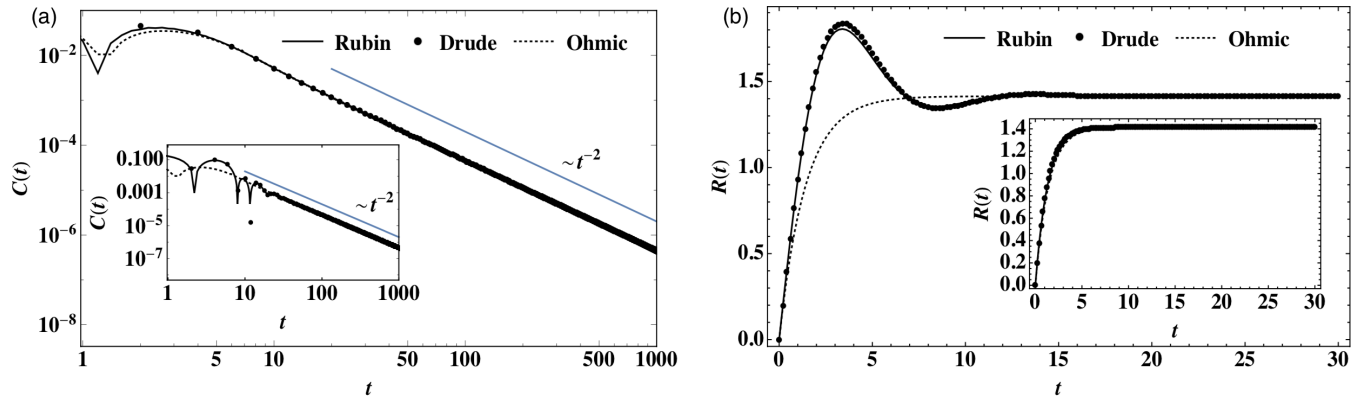


FIG. 10. (a) $C(t)$ at large times for $M = 1$, $m = 0.1$, $k = 5$, $k' = 4$, and $\beta = \infty$. Inset: The same plot for $k' = 0.5$. $C(t)$ behaves as $1/t^2$ as discussed in the text. (b) Comparison of the response function $R(t)$ between the three models for $M = 1$, $m = 0.1$, $k = 5$, $k' = 0.5$. Inset: The same plot for $k' = 4$. $R(t)$ saturates to the value $R_\infty = 1/\gamma_0 = 1/\sqrt{km} = 1.414$ [see Eq. (49)].

quantum-to-classical crossover time scales where the mean square displacement changes from a logarithmic to a linear time dependence. The analysis presented in this work provides a microscopic justification for the choice of the position response function used in a recent analysis [28] of quantum Brownian motion based on linear response theory as the starting point.

We have shown that the Ohmic limit, when the dissipation kernel becomes a δ function, is obtained in the limit of a continuum string and, surprisingly, for strong coupling. This is unlike the weak-coupling limits usually discussed in the derivation of quantum master equations in the literature [31,32]. An interesting observation is that at any finite temperature the noise correlations always have a finite correlation time even in the Ohmic limit when the dissipation kernel becomes a δ function. Thus a quantum bath is never truly Markovian. However, at high temperatures one can make the approximation $\coth(\beta\hbar\omega/2) \rightarrow 2/(\beta\hbar\omega)$ in the noise correlations and then get the Markovian limit. Thus our study shows

the precise conditions under which the Markovian approximation is valid. We note that the microscopic derivation of quantum master equations typically starts with exactly the same system-bath setup as the one used in the derivation of the quantum Langevin equation. There, the Born-Markov approximation leads to the Redfield equation and further approximations lead to the Lindblad equation, which is Markovian. The precise conditions for the validity of the Born-Markov approximation are subtle, however, and not clearly understood [31–33], and we believe that our work, with very explicit results, could provide insights into this issue.

ACKNOWLEDGMENTS

We acknowledge support by the Department of Atomic Energy, Government of India, under Project No. 12-R&D-TFR-5.10-1100. I.S. acknowledges the S.N. Bhatt Memorial Fellowship 2017 from the International Center for Theoretical Sciences.

-
- [1] P. Langevin, Sur la théorie du mouvement brownien, *C. R. Acad. Sci. (Paris)* **146**, 530 (1908).
 - [2] G. W. Ford, M. Kac, and P. Mazur, Statistical mechanics of assemblies of coupled oscillators, *J. Math. Phys.* **6**, 504 (1965).
 - [3] N. G. Van Kampen, *Stochastic Processes in Physics and Chemistry*, 3rd ed. (Elsevier, Amsterdam, 2007).
 - [4] U. Weiss, *Quantum Dissipative Systems*, 4th ed. (World Scientific, Singapore, 2012).
 - [5] P. E. Phillipson, Effects of long range interactions in harmonically coupled systems. I. Equilibrium fluctuations and diffusion, *J. Math. Phys.* **15**, 2127 (1974).
 - [6] V. Hakim and V. Ambegaokar, Quantum theory of a free particle interacting with a linearly dissipative environment, *Phys. Rev. A* **32**, 423 (1985).
 - [7] H. Grabert, P. Schramm, and G. L. Ingold, Quantum Brownian motion: The functional integral approach, *Phys. Rep.* **168**, 115 (1988).
 - [8] G. W. Ford, J. T. Lewis, and R. F. O’Connell, Quantum Langevin equation, *Phys. Rev. A* **37**, 4419 (1988).
 - [9] A. O. Caldeira and A. J. Leggett, Path integral approach to quantum Brownian motion, *Physica A* **121**, 587 (1983).
 - [10] R. P. Feynman and F. L. Vernon, The theory of a general quantum system interacting with a linear dissipative system, *Ann. Phys.* **24**, 118 (1963).
 - [11] R. Balescu, *Equilibrium and Nonequilibrium Statistical Mechanics* (John Wiley & Sons, New York, 1975).
 - [12] P. C. Hemmer, *Dynamic and Stochastic Types of Motion in the Linear Chain* (Norwegian Institute of Technology, Trondheim, 1959).
 - [13] P. Mazur and E. Montroll, Poincaré cycles, ergodicity, and irreversibility in assemblies of coupled harmonic oscillators, *J. Math. Phys.* **1**, 70 (1960).
 - [14] R. J. Rubin, Statistical dynamics of simple cubic lattices. model for the study of Brownian motion. II. *J. Math. Phys.* **2**, 373 (1961).
 - [15] R. E. Turner, Motion of a heavy particle in a one dimensional chain, *Physica* **26**, 269 (1960).

- [16] R. E. Turner, Temporal fluctuations in a classical linear system, *Physica* **26**, 274 (1960).
- [17] P. Mazur and E. Braun, On the statistical mechanical theory of Brownian motion, *Physica* **30**, 1973 (1964).
- [18] P. Ullersma, An exactly solvable model for Brownian motion: I. Derivation of the Langevin equation, *Physica* **32**, 27 (1966).
- [19] P. Ullersma, An exactly solvable model for Brownian motion: III. Motion of a heavy mass in a linear chain, *Physica* **32**, 74 (1966).
- [20] R. Zwanzig, Nonlinear generalized Langevin equations, *J. Stat. Phys.* **9**, 215 (1973).
- [21] C. Presilla, R. Onofrio, and U. Tambini, Measurement quantum mechanics and experiments on quantum zeno effect, *Ann. Phys.* **248**, 95 (1996).
- [22] C. Presilla, R. Onofrio, and M. Patriarca, Classical and quantum measurements of position, *J. Phys. A: Math. Gen.* **30**, 7385 (1997).
- [23] P. Hänggi and G. L. Ingold, Fundamental aspects of quantum Brownian motion, *Chaos: Interdisc. J. Nonlin. Sci.* **15**, 026105 (2005).
- [24] S. T. Smith and R. Onofrio, Thermalization in open classical systems with finite heat baths, *Eur. Phys. J. B* **61**, 271 (2008).
- [25] A. Lampo, M. G. March, and M. Lewenstein, *Quantum Brownian Motion Revisited: Extensions and Applications* (Springer, Berlin, 2019).
- [26] J. P. Eckmann, C. A. Pillet, and L. Rey-Bellet, Non-equilibrium statistical mechanics of anharmonic chains coupled to two heat baths at different temperatures, *Commun. Math. Phys.* **201**, 657 (1999).
- [27] S. Sinha and R. D. Sorkin, Brownian motion at absolute zero, *Phys. Rev. B* **45**, 8123 (1992).
- [28] U. Satpathi, S. Sinha, and R. D. Sorkin, A quantum diffusion law, *J. Stat. Mech.* **12**, 123105 (2017).
- [29] S. G. Das and A. Dhar, Landauer formula for phonon heat conduction: Relation between energy transmittance and transmission coefficient, *Eur. Phys. J. B* **85**, 372 (2012).
- [30] A. Chakraborty and R. Sensarma, Power-law tails and non-Markovian dynamics in open quantum systems: An exact solution from Keldysh field theory, *Phys. Rev. B* **97**, 104306 (2018).
- [31] H. J. Carmichael, *Statistical Methods in Quantum Optics 1: Master Equations and Fokker-Planck Equations* (Springer Science & Business Media, New York, 2013).
- [32] H. P. Breuer, F. Petruccione *et al.*, *The Theory of Open Quantum Systems* (Oxford University, Oxford, 2002).
- [33] A. Purkayastha, A. Dhar, and M. Kulkarni, Out-of-equilibrium open quantum systems: A comparison of approximate quantum master equation approaches with exact results, *Phys. Rev. A* **93**, 062114 (2016).